www.czasopisma.pan.pl PAN POLSKA AKADEMIA NAUK www.journals.pan.pl

Arch. Metall. Mater. **65** (2020), 3, 1005-1009

DOI: 10.24425/amm.2020.133207

NAMHYUK SEO[1], JUNHYUB JEON[1], SEUNGGYU CHOI[1],
YOUNG HOON MOON[2], IN-JIN SHON[1], SEOK-JAE LEE[1*]

MICROSTRUCTURAL AND MECHANICAL CHARACTERISTICS OF NON-EQUIATOMIC HIGH ENTROPY ALLOY FeMnCoCr PREPARED BY SPARK PLASMA SINTERING

In this study, a non-equiatomic high entropy alloy was fabricated using the spark plasma sintering method, and its microstructural features and mechanical properties were investigated. The chemical composition of FeMnCoCr was determined by using the entropy calculation related to the design of high entropy alloys. A bulk sample with the same composition was also prepared using the conventional metallurgical processes of casting and hot rolling. The microstructures of the samples fabricated by these different processes were compared by microscope observation, and a quantitative phase analysis was carried out using FE-SEM. Hardness measurement was used to evaluate mechanical properties. Particular attention was paid to microstructural changes due to heat treatment, which was analyzed by considering how austenite stability is affected by grain refinement.

Keywords: Non-equiatomic high entropy alloys; phase stability; heat treatment; micro-structural characteristics

1. Introduction

High entropy alloys were designed with similar atomic fractions of alloying elements, a different design concept compared to the design approach used for conventional alloys. High entropy alloys overcame the formation of intermetallic compounds and formed a single phase matrix such as body centered cubic (bcc) or face centered cubic (fcc) structure. These alloys have a high configurational entropy of mixing and serious lattice distortion due to equiatomic or near-equiatomic chemical compositions, resulting not only in outstanding mechanical properties, but also excellent high temperature and cryogenic temperature properties. These outstanding properties have made high entropy alloys the next generation of materials [1].

One of the typical roles for designing high entropy alloys has been to maximize the configurational entropy of mixing in order to achieve a single phase matrix [2]. However, recent studies have shown that configurational entropy is no longer a significant factor in creating a single phase, by removing the limitation of designing equiatomic compositions [3-5]. Researchers have instead proposed non-equiatomic high entropy alloys, which show dual phase or multi-phase formation in addition to single phase. The microstructure of mixed phases in non-equiatomic high entropy alloys has contributed very good mechanical properties [5,6]. In addition, weakness in price competitiveness for equiatomic high entropy alloys can be overcome by reducing the amounts of relatively expensive elements.

A key factor in the improvement in the mechanical properties of non-equiatomic high entropy alloys was the presence of some amounts of austenite phase at room temperature. The austenite phase contributed to improving mechanical properties during plastic deformation due to the transformation induced plasticity (TRIP) effect. The key factor is to control the stability of the austenite phase. Jimenez-Melero et al. have reported that grain refinement increased the stability of austenite in steels [7]. Oh et al. have found that the austenite stability of sintered iron-based alloys was increased by nano-sized crystallites [8]. Li et al. have reported that the shorter the annealing time, the smaller the grain size in a $Fe_{50}Mn_{30}Cr_{10}Co_{10}$ high entropy alloy. This caused the fraction of hexagonal closest packed (hcp) ε-phase to decrease and fcc phase to increase [9]. Previous investigations have determined that phase stability was influenced by both chemical composition and grain size. These studies were mostly carried out with bulk high entropy alloys fabricated by conventional process methods. However, few studies have investigated the relationship between austenite stability and grain size in high

[1] JEONBUK NATIONAL UNIVERSITY, DIVISION OF ADVANCED MATERIALS ENGINEERING, 567 BAEKJE-DAERO, DEOKJIN-GU, JEONJU, 54896, REPUBLIC OF KOREA
[2] PUSAN NATIONAL UNIVERSITY, SCHOOL OF MECHANICAL ENGINEERING, 2, BUSANDAEHAK-RO 63BEON-GIL, GEUMJEONG-GU, BUSAN, 46241, REPUBLIC OF KOREA

* Corresponding author: seokjaelee@jbnu.ac.kr

entropy alloys fabricated by the powder metallurgy process. Accordingly, we prepared the non-equiatomic high entropy alloy $Fe_{50}Mn_{30}Co_{10}Cr_{10}$ [5] using the powder metallurgy process and investigated the relationship between austenite stability and heat treatment conditions.

2. Experimental

Fe-25%Mn-20%Co-10%Cr (in at.%) alloy was designed in the present study. The amount of Mn, a known austenite stabilizing element, was reduced, while the amount of Co, a stabilizing element of bcc phase in high entropy alloys, was increased in comparison to the FeMnCoCr alloy used in a previous work [10]. Fe powder (Höganäs AB, purity of 99.9%, average particle size of <75 μm), Mn powder (Alfa Aesar, purity of 99.6%, average particle size of <10 μm), Co powder (Alfa Aesar, purity of 99.8%, average particle size of 1.6 μm), and Cr powder (Alfa Aesar, purity of 99%, average particle size of <140 μm) were weighted to prepare the FeMnCoCr alloy sample. A high-energy ball milling (a Pulverisette-5 planetary mill) under Ar atmosphere with ball to powder ratio of 30:1 was carried out for 24 hours at 250 rpm for the mechanical milling. Spark plasma sintering (SPS) was adopted to prepare the sintered FeMnCoCr alloy sample. The mechanically milled alloy powder was sintered at a rate of 1000°C/min under Ar atmosphere with uniaxial pressure of 80 MPa during sintering, followed by air cooling at room temperature. The bulk FeMnCoCr alloy sample was obtained by following conventional casting and hot-rolling procedures. The raw material was melted at a temperature of 1500°C under vacuum atmosphere in a high frequency induction melting furnace (ELTeK Co. LTD, HF-50K). The bulk specimen was deformed by approximately 50% at 900°C by hot rolling. Specimens prepared respectively by the sintering process (SP) and hot rolling (HR) were annealed at 900~1000°C for 1 to 2 hrs. in a tubular furnace (Lenton Co., LTF-15/50/450), and then rapidly cooled by water. Phase change was analyzed by X-ray diffraction (XRD) at 40 kV and 30 mA with a Cu Kα target (Shimadzu, XRD-6100). XRD samples were analyzed over the 2θ range of 40-120° with 4°/min scan speed. The composition of the specimens and microstructure were analyzed by energy dispersive spectrometry (EDS) and electron backscatter diffraction (EBSD) using a field emission scanning electron microscope (FE-SEM, HITACHI, SU-70). The EBSD samples were mechanically polished and etched by colloidal solution. Mechanical properties were evaluated with a Micro Vickers hardness tester (Mitutoyo Co., TH715). The test was carried out 5 times for each sample. And, the mean and standard deviation of the excluding maximum and minimum values were used for the evaluation. To calculate the average and standard deviation of the excluding maximum and minimum values.

3. Results and discussion

Fig. 1 shows XRD analysis results, which confirm the peaks of α, γ, and ε phases both in the HR and SP specimens. This means that the alloy samples were well synthesized. The HR specimens showed high peak intensities for α and ε phases while the SP specimens showed strong austenite γ peaks. It was anticipated that the SP specimens would be synthesized in the γ phase due to the highly small grains formed during the powder metallurgy process. The intensities of each peak varied after the annealing treatment.

To compare the volume fraction of each phase, an EBSD image was quantitatively analyzed. Volume fraction of phases varied according to the different heat treatment conditions in the HR specimens, whose EBSD images are compared in Fig. 2. Before annealing, the HR specimens indicate 85.8 vol.% ε phase (blue color), 11.5 vol.% α phase (red color), and 2.7 vol.% vol-

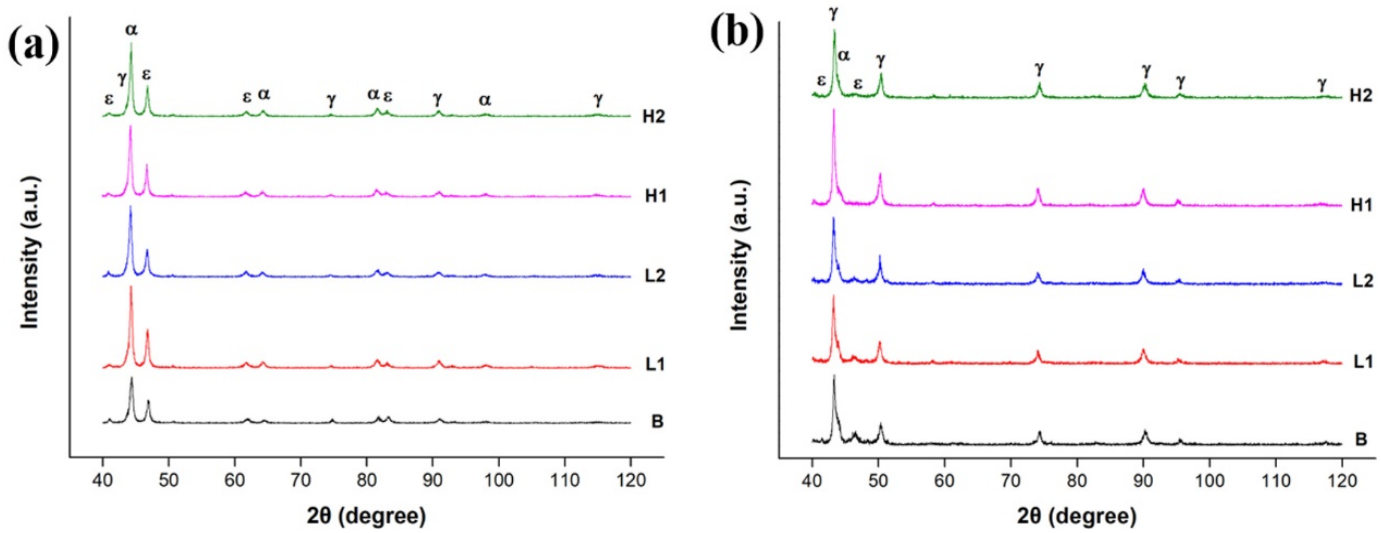

Fig. 1. XRD patterns of the (a) HR and (b) SP specimens under different heat treatment conditions. B denotes the specimen before annealing, L1 deontes the specimen annealed at 900°C for 1 h, L2 denotes the specimen annealed at 900°C for 2 h, H1 denotes the specimen annealed at 1000°C for 1 h, and H2 denotes the specimen annealed at 1000°C for 2 h

ume of γ phase (green color). The volume fraction of the ε phase decreases and that of the α phase increases relatively, while that of the γ phase shows a slight increase after annealing at 900°C. These phase changes are believed to be caused by recrystallization phenomenon. Li et al. have reported that a reduction in the hcp ε phase was observed in the C added $Fe_{50}Mn_{30}Co_{10}Cr_{10}$ alloy [11], which was related to the recrystallization that occurred during annealing. When the HR specimen is annealed at 1000°C, the volume fraction of the ε phase decreases and those of the α and γ phases increase together. The volume fraction of the α phase increases noticeably after annealing but there is no variation that depends on annealing temperature. The volume fraction of the γ phase is markedly increased as the HR specimen is annealed at a high temperature of 1000°C. In general, austenite stability decreases as grain size increases. The average size of grains should increase as the annealing temperature increases, since grain growth is a diffusion controlled phenomenon, resulting in decreased volume fraction of the γ phase. However, a higher volume fraction of the γ phase is observed in the HR specimen annealed at 1000°C, as seen in Fig. 2. Two possible reasons may account for this. Grain boundaries are preferred nucleation sites for phase transformations, i.e., bcc α martensite transformed from fcc γ austenite [12]. For this reason, it is believed that the transformation of the γ phase progresses more rapidly and grain growth accelerates concurrently, at a higher annealing temperature of 1000°C, while decomposition of the γ phase during cooling is delayed due to the reduced number of nucleation sites. It has also been reported that fine grains interfere with the slide of dislocations required for ε phase formation [13].

The volume fractions of phases varied with different heat treatment conditions in the SP specimens, and their EBSD images are compared in Fig. 3. Even though the volume fraction of the γ phase in the SP specimen before annealing is much higher

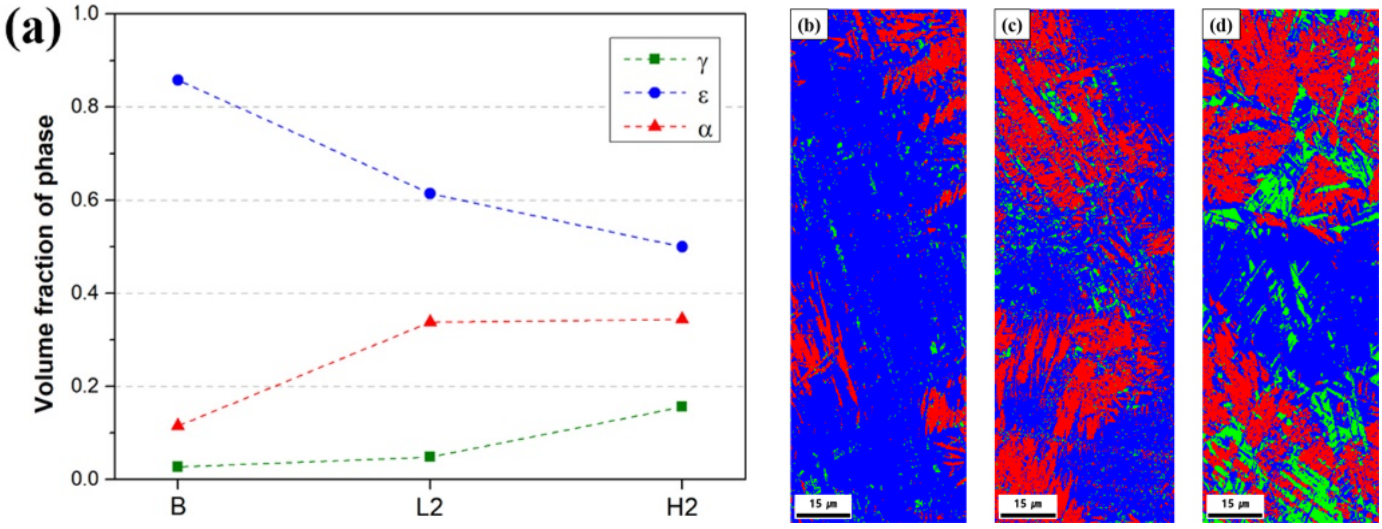

Fig. 2. (a) Volume fractions of phases changed by heat treatment conditions in the HR specimens and EBSD images for different specimens: (b) before annealing, (c) annealed at 900°C for 2 h, and (d) annealed at 1000°C for 2 h.

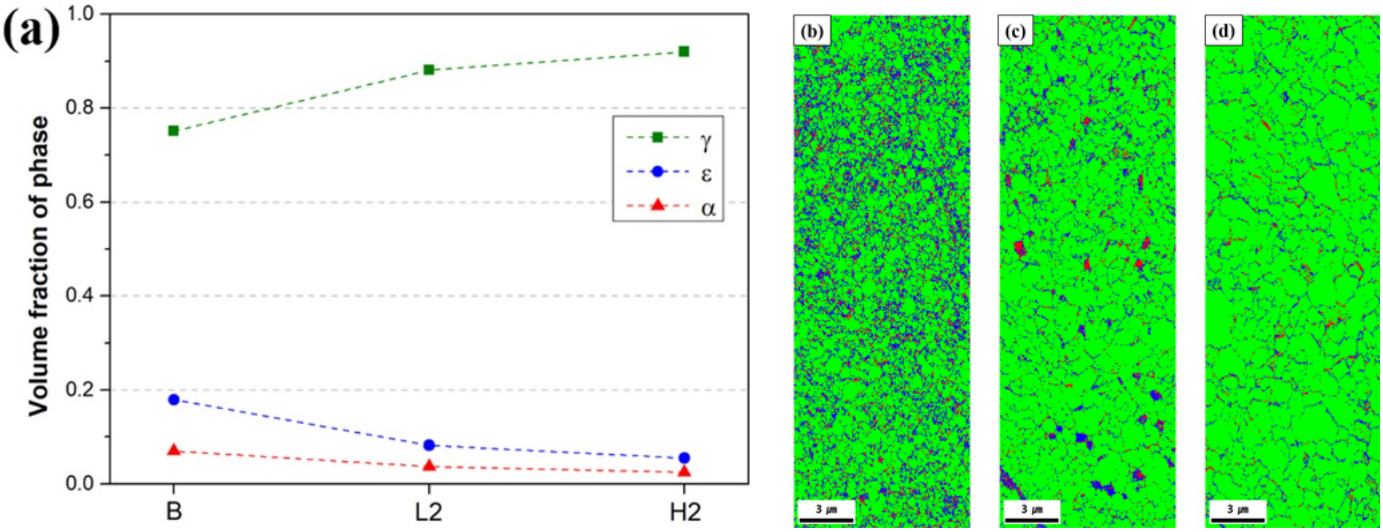

Fig. 3. (a) Volume fractions of phases changed by heat treatment conditions in the SP specimens and EBSD images for different specimens: (b) before annealing, (c) annealed at 900°C for 2 h, and (d) annealed at 1000°C for 2 h

than that in the HR specimen, it is observed that the volume fraction of the γ phase in the SP specimen gradually increases as the SP specimen is annealed at a higher temperature. Annealing at higher temperatures may lead to a higher volume fraction of γ phase being transformed during the annealing process itself; it may also slow the decomposition of the γ phase during cooling, owing to the reduced number of nucleation sites resulting from grain boundaries.

Fig. 4 compares phase fractions of HR and SP specimens under different heat treatment conditions. Regardless of annealing conditions, the volume fraction of γ phase in the SP specimen is significantly higher than that in the HR specimen. The maximum volume fraction of γ phase is less than 20 vol.% in the bulk FeMnCoCr alloy, but we achieved almost 90 vol.% of γ phase in the same FeMnCoCr alloy fabricated by the powder metallurgy method a highly significant result. The presence of γ phase in Fe-based alloys is essential to improving mechanical properties by anticipating the transformation induced plasticity (TRIP) effect during deformation [14]. Addition of a large amount of alloying elements such as Ni or Mn is a common way to produce a meaningful volume fraction of γ phase at room temperature. A very high volume fraction of γ phase in a non-equiatomic FeMnCoCr high entropy alloy was successfully achieved by sintering, without the need for additional austenite stabilizing elements.

Fig. 5 shows hardness values varied with heat treatment conditions in the HR and SP specimens. Hardness values in the SP specimens are more than double those in the HR specimens, irrespective of the heat treatment conditions. This is clearly due to the Hall-Petch relationship [15]; the smaller the grain size, the higher the strength. It seems that the decrease in hardness as annealing time increases is caused by the progress of recrystallization and grain growth [16].

4. Conclusions

Bulk and sintered non-equiatomic FeMnCoCr high entropy alloy specimens were fabricated using conventional and powder metallurgy methods respectively. The volume fraction of α phase was increased mainly by decreasing that of ε phase after annealing of the HR specimens. A γ phase volume fraction exceeding 75 vol.% could be achieved in the SP specimens before annealing, and γ phase volume fraction was maximized after annealing at 1000°C. The sintered FeMnCoCr specimens with remarkably smaller grains resulted in a hardness increment

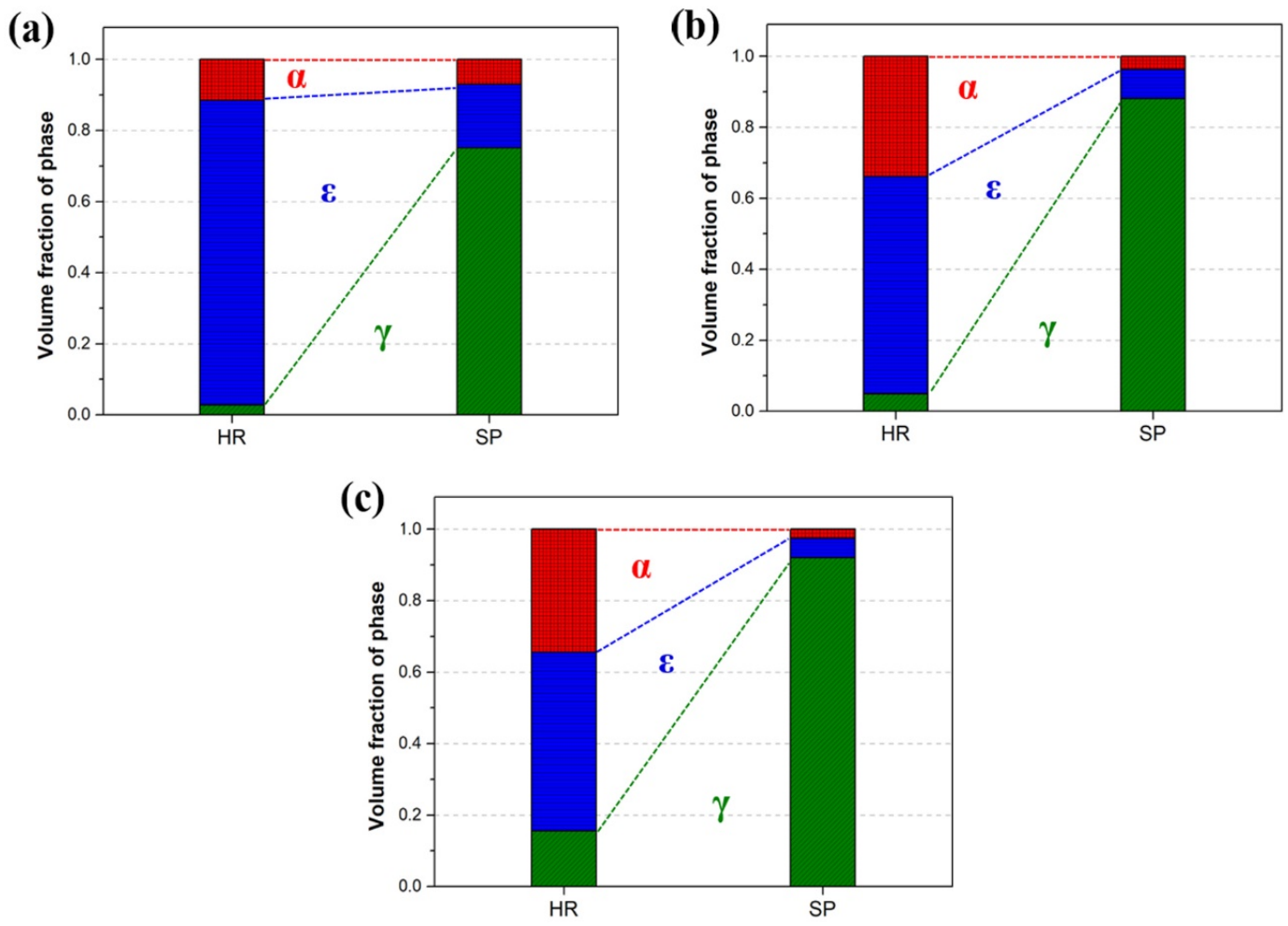

Fig. 4. Comparison of phase fractions for each heat treatment condition: (a) before annealing, (b) annealed at 900°C for 2 h, and (c) annealed at 1000°C for 2 h

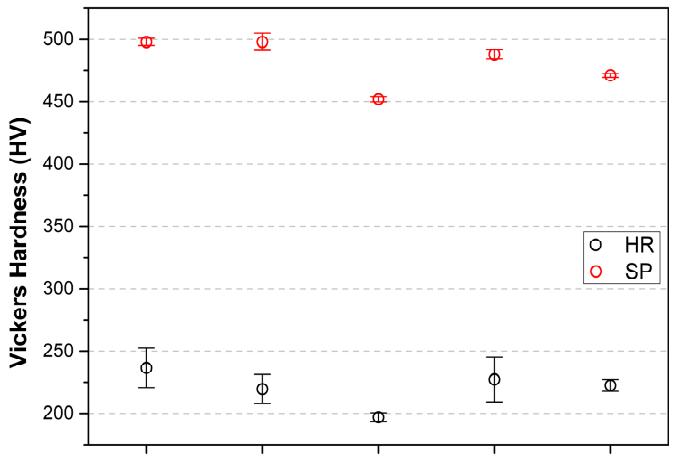

Fig. 5. Variation in hardness values depending on heat treatment conditions

more than double that of the FeMnCoCr specimens fabricated by conventional hot rolling. Differences in grain size affected not only the stability of γ austenite but also recrystallization during annealing and phase transformation during cooling.

Acknowledgments

This research was supported by the Basic Science Research program through the National Research Foundation of Korea (NRF) funded by the Ministry of Education (2016R1A1B03935163). It was also financially supported by the Ministry of Trade, Industry and Energy (MOTIE) and the Korea Institute for Advancement of Technology (KIAT) through the International Cooperative R&D program (P006837).

REFERENCES

[1] D. Yim, H.S. Kim, Korean J. Met. Mater. **55**, 671 (2017).
[2] J.W. Yeh, S.K. Chen, S.J. Lin, J.Y. Gan, T.S. Chin, T.T. Shun, C.H. Tsau, S.Y. Chang, Adv. Eng. Mater. 6, 299 (2004).
[3] Y.P. Wang, B.S. Li, H.Z. Fu, Adv. Eng. Mater. 11, 641 (2009).
[4] C.C. Tasan, Y. Deng, K.G. Pradeep, M.J. Yao, H. Springer, D. Raabe, JOM **66**, 1993 (2014).
[5] Z. Li, D. Raabe, JOM 69, 2099 (2017).
[6] D. Raabe, C.C. Tasan, H. Springer, M. Bausch, Steel Res. Int. **86**, 1127 (2015).
[7] E. Jimenez-Melero, N.H. van Dijk, L. Zhao, J. Sietsma, S.E. Offerman, J.P. Wright, S. van der Zwaag, Scr. Mater. **56**, 421 (2007).
[8] S.J. Oh, D. Park, K. Kim, I.J. Shon, S.J. Lee, Mater. Sci. Eng. A **725**, 382 (2018).
[9] Z. Li, C.C. Tasan, K.G. Pradeep, D. Raabe, Acta Mater. **131**, 323 (2017).
[10] H. Song, D.G. Kim, D.W. Kim, M.C. Jo, Y.H. Jo, W. Kim, H.S. Kim, B.J. Lee, S. Lee, Sci. Rep. **9**, 6163 (2019).
[11] Z. Li, C.C. Tasan, H. Springer, B. Gault, D. Raabe, Sci. Rep. **7**, 40704 (2017).
[12] S.J. Lee, Y.K. Lee, Mater. Sci. Forum **475-479**, 3169 (2005).
[13] J.H. Jun, C.S. Choi, Mater. Sci. Eng. A, **257**, 353 (1998).
[14] J. Chiang, B. Lawrence, L.D. Boyd, A.K. Pilkey, Mater. Sci. Eng. A **528**, 4516 (2011).
[15] H. Kotan, M. Saber, C.C. Koch, R.O. Scattergood, Mater. Sci. Eng. A **552**, 310 (2012).
[16] C.S. Choi, I.J. Shon, J. Met. Mater. **25**, 492 (1987).